

## Exploding-Foil Technique for Achieving a Soft X-Ray Laser

M. D. Rosen, P. L. Hagelstein, D. L. Matthews, E. M. Campbell, A. U. Hazi, B. L. Whitten,  
B. MacGowan,<sup>(a)</sup> R. E. Turner, and R. W. Lee

*Lawrence Livermore National Laboratory, University of California, Livermore, California 94550*

and

G. Charatis, Gar. E. Busch, C. L. Shepard, and P. D. Rockett

*KMS Fusion, Inc., Ann Arbor, Michigan 48106*

(Received 26 October 1984)

We describe a design for producing a soft x-ray laser via  $3p$ - $3s$  transitions in Ne-like selenium (wavelength of about 200 Å). A 0.53- $\mu\text{m}$  laser, focused in a  $1.2 \times 0.02$ -cm spot to  $\sim 5 \times 10^{13}$  W/cm<sup>2</sup>, heats and burns through a thin foil of Se. Besides ionizing the Se to a Ne-like state, the laser explodes the foil, creating a region of uniform electron density. This allows propagation of the x rays down the 1-cm-long gain direction without debilitating refraction. Gains of 4 to 10 cm<sup>-1</sup> are predicted for various transitions.

PACS numbers: 42.60.By, 32.30.Rj, 32.70.-n, 52.50.Jm

For ions in the neon isoelectronic sequence, the rates for electron collisional excitation from the  $1s^2 2s^2 2p^6$  ground-state configuration to  $1s^2 2s^2 2p^5 3p$  are greater than the rates for excitation from the ground state to  $1s^2 2s^2 2p^5 3s$ . Whereas the  $2p^5 3p$   $J=0$  levels are populated by direct monopole excitation from the ground state, other  $2p^5 3p$  levels such as  $J=2$  are fed primarily by cascades from upper levels and recombination from F-like ions. Dipole radiative decay of the  $2p^5 3p$  levels to the ground state is forbidden, while the  $2p^5 3s$   $J=1$  levels radiatively decay very rapidly, leading to population inversion between the  $3p$  and  $3s$  levels. (See Fig. 1.) For electron densities and temperatures that are typical of laboratory laser-produced plasmas, calculations<sup>1-6</sup> have shown that under favorable conditions large soft x-ray laser gains and amplification can be achieved.

From theoretical considerations,<sup>5</sup> the most promising elements in which to implement this laser-driven electron-collisional-excitation scheme, occur near  $Z=36$ . Therefore solid Se ( $Z=34$ ) was chosen as a candidate material. Elements much lower in  $Z$  tend to overionize, and those with higher  $Z$  have lower excitation rates for  $n=2$  to  $n=3$  transitions. Reference 5 describes the predicted high gains at 183 Å [ $(2p_{1/2}^5 3p_{1/2})_{J=0}$  to  $(2p_{1/2}^5 3s_{1/2})_{J=1}$ ] when 0.53  $\mu\text{m}$  light, line focused at an intensity of  $10^{14}$  W/cm<sup>2</sup>, illuminates solid Se. In that approach, the high-gain region occurs along the steep density gradient caused by the laser-heated blowoff from the Se surface. The lack of an observed signal in previous experiments<sup>7</sup> was attributed<sup>5</sup> to refraction (due to the steep gradient) which bends the x-rays out of the high-gain region (thus preventing significant amplification) and out of the line of sight of the diagnostic instruments.

In this paper we present a technique designed to minimize the refraction problem while still producing

plasma conditions suitable for lasing. The target is a thin Se foil, typically 750 Å deposited on 1500 Å of Formvar (polyvinyl formal, C<sub>11</sub>H<sub>18</sub>O<sub>5</sub>) for structural integrity. The 0.53- $\mu\text{m}$  laser is focused by a cylindrical lens to a 1.2-cm-long by 0.02-cm-wide region of the foil. The foil explodes as the laser burns through it, creating a rather uniform electron density in the plasma that has expanded into a roughly cylindrical shape. The uniformity allows the x-ray laser beam to proceed straight down the long line focus direction, stay within the region of high gain, and propagate into the narrow angle of acceptance of the diagnostics. Exploding foils have previously been used<sup>8</sup> to create large-scale-length plasmas to study laser-driven parametric instabilities.

There are two main tools employed in the design of the foils. The two-dimensional (2D) code LASNEX<sup>9</sup> simulates the laser-foil interaction, including absorption, burnthrough, and hydrodynamic motion. It has been exercised with great success in dealing with other high- $Z$ , non-local-thermodynamic-equilibrium laser-created plasmas.<sup>10</sup> Quantities such as the time-evolving electron and ion temperatures, densities, and flow fields are then fed into the 2D x-ray-laser code XRASER.<sup>5</sup> XRASER uses this input (along with detailed atomic data computed off-line) to calculate level populations and gain as a function of space and time. The atomic model includes in detail all the singly excited states of the Ne-like and Na-like ions with  $n=3$  and 4 and F-like ions with  $n=2$  and 3. Simpler models were used for the other sequences and levels. For the  $n=2$  to 3,4 transitions, collisional excitation cross sections were computed by use of a multiconfiguration, relativistic, distorted-wave code.<sup>11</sup> Line transfer is computed in 1D and 2D including the effects of partial redistributions and bulk Doppler shifts, with use of a modified  $S_n$  (ray) algorithm with a linearized convergence scheme for an equivalent two-level atom. In

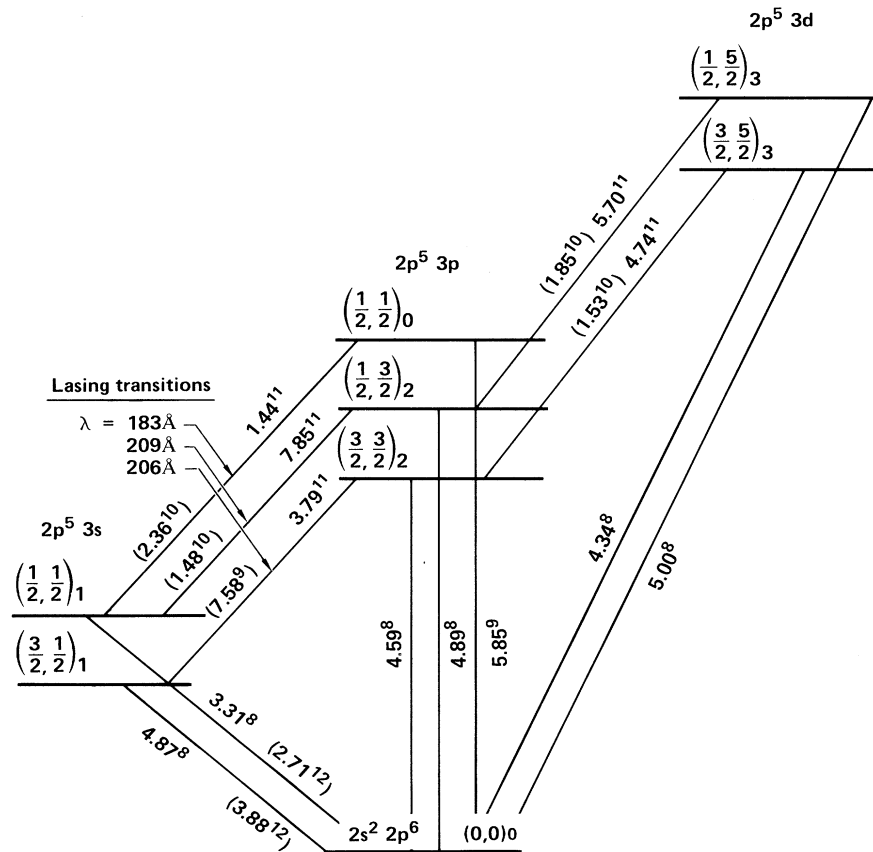


FIG. 1. Simplified energy-level diagram [( $j_1, j_2$ ) $_j$  notation] for Ne-like Se. (Hundreds of levels are included in the calculations.) Collisional excitation rates and radiative decay rates (in parentheses) for  $n_e = 5 \times 10^{20} \text{ cm}^{-3}$  and  $T_e = 1 \text{ keV}$  are shown.

particular, trapping between the ground state and the  $3s$  and  $3d$  levels are included, as they can affect the predicted gain to a moderate degree. A postprocessor SPECTRE produces a predicted spectrum for any particular line of sight, including (in 1D) refraction effects, to facilitate direct comparison with experimental data.

The design goal is to produce a flat electron density ( $n_e$ ) and temperature profile, with scale length  $L$  of at least  $100 \mu\text{m}$ , to last at least  $100 \text{ ps}$ , with high enough  $n_e$  ( $\sim 5 \times 10^{20} \text{ cm}^{-3}$ ) for appreciable density of neon-like ions and gain. These numbers are motivated by simple considerations. For a linear density gradient,  $n_e = n_0[1 - (y/L)]$ , an x-ray propagating in the  $x$  direction has a trajectory  $y = x^2 d/4L$ , where  $d = \omega_{p0}^2/\omega^2 = 1/2500$  for  $n_0 = 10^{21} \text{ cm}^{-3}$  and a  $50\text{-eV}$  x ray. For a typical  $10\text{-mrad}$  divergence and acceptance angle of the spectrograph, and an  $x = 1\text{-cm}$  line focus,  $y = 0.01 \text{ cm}$ , which leads to the  $L = 0.01\text{-cm}$  requirement. The transit time for the x-rays down the the  $1.2 \text{ cm}$  is about  $40 \text{ ps}$ , which leads to the requirement of a  $100 \text{ ps}$  or so duration of the plasma. A two-sided Novette laser illumination of the foil (1 beam per side) is employed in an attempt to compensate for random

nonuniformities in any one beam that could lead to refractory density nonuniformities in the lasing medium. However, as will be shown below, even a 1-beam illumination is sufficient to explode the foil nearly symmetrically, so that with a sufficiently smooth beam profile it also would be an acceptable illumination scheme.

Experiments were performed at KMS Fusion, Inc., to test the LASNEX and XRASER modeling of the exploding foil, with use of a single beam of  $0.53\text{-}\mu\text{m}$  laser light. A  $0.26\text{-}\mu\text{m}$  probing laser of  $20 \text{ ps}$  duration produces holographic interferograms which can be inverted to indicate density profiles of the plasma.<sup>12</sup> In Fig. 2 we see the results from a  $5 \times 10^{13}\text{-W/cm}^2$ ,  $360\text{-ps}$  flat-topped illumination of a Se on Formvar foil, probed about  $100 \text{ ps}$  after the end of the pulse. The LASNEX simulation matches the data fairly well. Note the nearly symmetric profile despite the single-sided illumination, and the flat  $n_e$  profile over the requisite  $100\text{-}\mu\text{m}$  distance. We have no data, however, on turbulence that may affect the density profile on the scale of  $1 \mu\text{m}$  or shorter. The code's predictions track the profile data over large variations in intensity, pulse

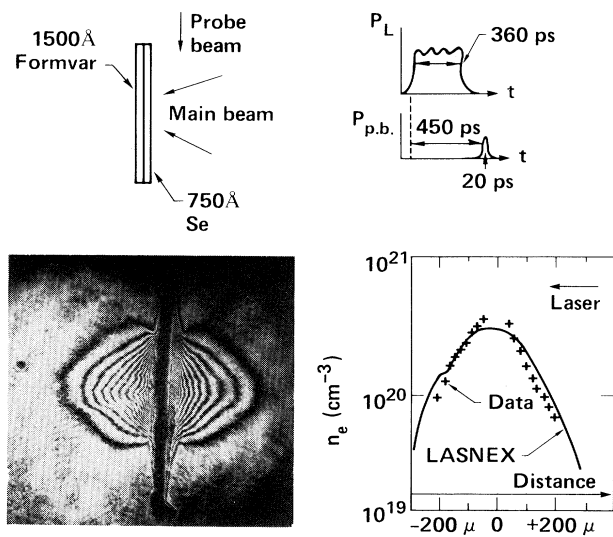


FIG. 2. Experimental setup for, and example of, holographic interferometry, along with comparison of LASNEX simulation (solid line) and electron density profile (crosses) inferred from the Abel inversion of the interferogram.

length, and probing times, leading to substantial confidence in this aspect of the modeling.

An inference of the electron temperature  $T_e$  can be made by observing the light scattered  $135^\circ$  from the incident laser's  $k$  vector at wavelengths between 0.53 and  $1.06 \mu\text{m}$ . The detected spectrum is interpreted<sup>13</sup> in terms of stimulated Raman scatter (SRS). The short-wavelength cutoff of this SRS spectrum is usually quite sharp, and is attributed to Landau damping at  $k_e \lambda_D = 0.3$ , where  $k_e$  is the wave number of the electron-plasma wave, and  $\lambda_D$  is the Debye length. In the Novette experiments on the actual x-ray-laser thin-foil targets, most of the data show spectral cutoffs ranging from 0.67 to  $0.70 \mu\text{m}$ , leading to estimates of peak  $T_e$  in the 700 to 1000 eV range. This is in rather close agreement to the predicted  $T_e$  of 900 eV. (The ion temperature is predicted to be about 400 eV). In addition, dot spectroscopy,<sup>14</sup> with use of the  $\text{Si}^{13+}(\text{Ly}_\alpha)$ -to- $\text{Si}^{12+}(\text{He}_\alpha)$  ratio as a  $T_e$  diagnostic, has been used to infer the plasma temperature in Se-disk experiments at KMS. Preliminary analysis indicates that the results agree with the predictions of LASNEX.

Given the densities and temperatures from LASNEX, XRASER predicts the fraction of Se in various ionization states. While most of the excitation and ionization rates and their inverses are calculated from first principles,<sup>3,11</sup> dielectronic recombination is modeled in a crude way, albeit with plausible gross rates of  $(1-5) \times 10^{-11} \text{ cm}^3 \text{ sec}^{-1}$ . In Fig. 3 a theoretical 3s-2p and 3d-2p spectrum is compared to one obtained from a KMS experiment. In this case the thin foil was illuminated with a 1-mm line focus at  $5 \times 10^{13} \text{ W/cm}^2$

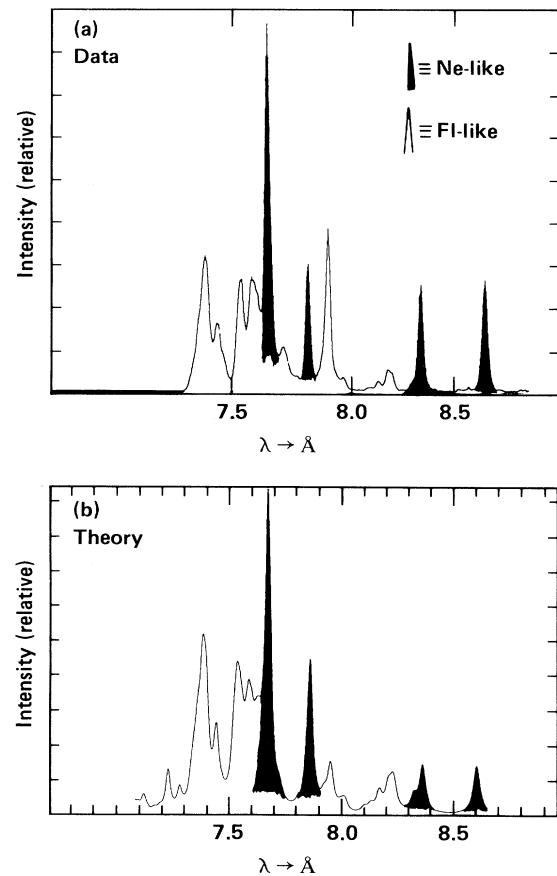


FIG. 3. Comparison of (a) experiment and (b) theory for the time resolved 3-2 spectra of Se. Darkened lines are Ne-like, and undarkened lines are F-like. Time is near the peak of the pulse. Lines above 8 Å are 3s-2p, and below 8 Å are 3d-2p.

and the data are time resolved, but spatially integrated over the exploding foil. Since the  $n_e$  and  $T_e$  profiles are quite uniform, the spatial integration does not severely compromise the data. The 3d-2p parts of the spectrum show rather good agreement with the theory, though the modeling perhaps overpredicts the F-like fraction by a moderate amount. The simulations predict about 30% of the Se to be the Ne-like, and about 40% F-like. The 3s-2p lines are quite a bit stronger than the theory's predictions.

The gains are predicted to be largest in the roughly 200- $\mu\text{m}$ -diam, nearly cylindrical, uniform-density, central part of the exploding foil. This foil was irradiated at  $4 \times 10^{13} \text{ W/cm}^2$  for 450 ps. The predicted gain for the  $J = 0$  to 1 transition at 183 Å at the peak of the pulse is about  $10 \text{ cm}^{-1}$ . Before the peak of the optical-laser pulse, the foil has not burned through and refraction interferes with the x-ray propagation. By about 200 ps after the peak of the pulse the foil has expanded and cooled significantly. The lowered density

contributes to a falling gain, as does the drop in mono-pole excitation rate due to the cooling. The predicted gain for a  $J=2$  to 1 transition [ $(2p_{1/2}^5 3p_{3/2})_{J=2}$  to  $(2p_{1/2}^5 3s_{1/2})_{J=1}$ ] at 209 Å is about  $4 \text{ cm}^{-1}$ . The gain stays slightly more constant in time for the  $J=2$  lines, since those levels are fed by cascading from higher levels during the cooling phase. Similar gains are predicted for the  $(2p_{3/2}^5 3p_{3/2})_{J=2}$  to  $(2p_{3/2}^5 3s_{1/2})_{J=1}$  transition at 206 Å.

The measured gains are described in the companion paper.<sup>15</sup> While the  $J=2$  to 1 transitions exhibit amplification with a gain coefficient of about  $5 \pm 1 \text{ cm}^{-1}$ , within 50% of our predictions here, the  $J=0$  to 1 transition is not observed to amplify to any great degree, and certainly not within an order of magnitude of the predicted  $10 \text{ cm}^{-1}$ . The time behavior of the  $J=2$  to 1 lasing lines follows the theory rather closely, lending credence to the physical picture presented above. The agreement of the  $J=2$  gain to within 50% of the theory is as good as we can reasonably expect, given our uncertainties in  $n_e$ ,  $T_e$ , and in the fraction of the Se in the Ne-like state. It is of interest to note that the  $J=2$  to 1 transitions at 206 and 209 Å are both calculated and measured to have nearly equal gains. This equality appears to be remarkable coincidence and should not necessarily be expected in other systems, as evidenced by the shorter-wavelength lasing results with a higher- $Z$  element yttrium.<sup>15</sup> We believe that Ni-like states (which use higher- $Z$  elements) can also lead to lasing<sup>16</sup> of the type discussed here, possibly with higher gain, and at shorter wavelengths.

There are many speculations as to the absence of the  $J=0$  to 1 laser. The collisional-excitation rate directly into the state has been calculated by numerous authors<sup>3,4,6,17</sup> and all agree fairly closely. Extra recombinative processes may be feeding the lower ( $3s$ ) levels as well as the  $J=2$   $3p$  levels, thus maintaining the  $J=2$  inversion while destroying the  $J=0$  one. (This harkens back to the high  $3s$ - $2p$  emission discussed earlier.) Another way to destroy the  $J=0$  inversion is to mix the  $3p$  manifold such that all the sublevels are populated according to their statistical weights (the sublevels are less than 10-eV apart, and are in a 1-keV plasma). We have not identified the actual mechanisms to date. Varying  $Z$  did not produce the missing laser either, thus virtually ruling out coincidental absorption resonances. Another way to deplete the  $J=0$  level may be electron capture. Consider a state with an electron already in the  $3p$   $J=0$  level. Electron capture promotes another electron from the  $L$  shell into a higher-lying Rydberg level. The principal decay mode of this three-excited-electron state is the transfer of the  $3p$  electron to the  $L$  shell (thus depleting  $J=0$ ), release of the captured free electron, and the eventual cascade of the previously promoted  $L$ -shell electron back down to lower levels, quite possibly the  $J=2$  levels.

In summary, data from holography, Si-dot and Raman spectroscopy, and 3-2 Se spectroscopy give us some confidence that the exploding foil plasma has been prepared in roughly the way the modeling would predict. To produce gain, amplification, and propagation we have created a flat  $n_e$  ( $5 \times 10^{20} \text{ cm}^{-3}$ ) and  $T_e$  (1 keV) profile, with a substantial fraction of the Se in a Ne-like state. Gain predictions for the  $J=2$  to 1 transitions are within 50% of the observations, but we can only speculate as to the fate of the missing  $J=0$  to 1 transition.

We gratefully acknowledge the help and support of many colleagues in this effort. In particular, J. Nuckolls, T. Weaver, J. Lindl, R. London, and S. Maxon for target design; W. Kruer, K. Estabrook, and B. Lasinski for laser-plasma interactions; S. Morgan and J. Scofield for atomic physics; L. Minner, R. Jung, and M. Runyan for XRASER code support. This work was performed under the auspices of the U. S. Department of Energy under Contract No. W-7405-ENG-48.

(a)Permanent address: Blackett Laboratory, Imperial College, SW7 2AZ London, United Kingdom.

<sup>1</sup>A. N. Zherikhin, K. N. Koshelev, and V. S. Letokhov, *Sov. J. Quantum Electron.* **6**, 82 (1976).

<sup>2</sup>A. V. Vinogradov and V. N. Shylaptsev, *Sov. J. Quantum Electron.* **13**, 1511 (1983), and references therein.

<sup>3</sup>P. L. Hagelstein, Ph.D. thesis, Lawrence Livermore National Laboratory Report No. UCRL-53100, 1981 (unpublished).

<sup>4</sup>U. Feldman, A. K. Bhatia, and S. Suckewer, *J. Appl. Phys.* **54**, 2188 (1983).

<sup>5</sup>P. L. Hagelstein, *Plasma Phys.* **25**, 1345 (1983).

<sup>6</sup>U. Feldman, J. F. Seely, and A. K. Bhatia, *J. Appl. Phys.* **56**, 2475 (1984), and references therein.

<sup>7</sup>D. Matthews *et al.*, in Proceedings of the IEEE Second Topical Meeting on Laser Techniques in the Extreme Ultraviolet, Boulder, Colorado, March 1984 (to be published).

<sup>8</sup>D. W. Phillion, E. M. Campbell, K. G. Estabrook, G. E. Phillips, and F. Ze, *Phys. Rev. Lett.* **49**, 1405 (1982).

<sup>9</sup>G. B. Zimmerman, Lawrence Livermore National Laboratory Report No. UCRL-75881, 1974 (unpublished); G. B. Zimmerman and W. L. Kruer, *Comments Plasma Phys. Controlled Fusion* **2**, 85 (1975).

<sup>10</sup>M. D. Rosen *et al.*, *Phys. Fluids* **22**, 2020 (1979); W. C. Mead *et al.*, *Phys. Fluids* **26**, 2316 (1983).

<sup>11</sup>P. L. Hagelstein and R. Jung, unpublished.

<sup>12</sup>M. D. Rosen *et al.*, *Bull. Am. Phys. Soc.* **27**, 989 (1982); W. B. Fechner *et al.*, *Phys. Fluids* **27**, 1552 (1984).

<sup>13</sup>R. E. Turner *et al.*, to be published.

<sup>14</sup>M. J. Herbst *et al.*, *Rev. Sci. Instrum.* **53**, 1418 (1982).

<sup>15</sup>D. L. Matthews *et al.*, following Letter [*Phys. Rev. Lett.* **54**, 110 (1985)].

<sup>16</sup>S. Maxon, P. Hagelstein, K. Reed, and J. Scofield, *J. Appl. Phys.* (to be published).

<sup>17</sup>K. Reed and A. U. Hazi, Lawrence Livermore National Laboratory Report No. UCRL-87014 (unpublished).

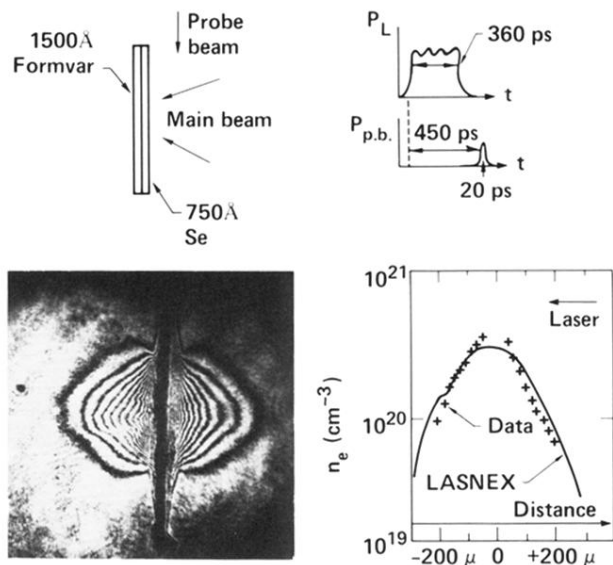


FIG. 2. Experimental setup for, and example of, holographic interferometry, along with comparison of LASNEX simulation (solid line) and electron density profile (crosses) inferred from the Abel inversion of the interferogram.